CRYSTAL GROWTH & DESIGN

pubs.acs.org/crystal

Article

Tolerance Factor and Phase Stability of the Normal Spinel Structure

Zhen Song and Quanlin Liu*

Cite This: *Cryst. Growth Des.* 2020, 20, 2014–2018

Read Online

ABSTRACT: Tolerance factor for the normal-spinel structure is introduced as a structural descriptor to predict the phase stability. It is derived following similar principles as those of perovskite and garnet structures, i.e., the geometrical relationship between multitype polyhedra. The calculation of tolerance factor only requires the ionic radii of compositional components involved. A survey of the tolerance factor over 120 AB_2X_4-type compounds proves the reliability. The numerical values are distributed below 1, which originates from the compressed octahedra which support the framework of spinel. The tolerance factor will be helpful in machine learning and high-throughput screening methods for fast evaluation of phase stability and materials properties of spinel-type compounds.

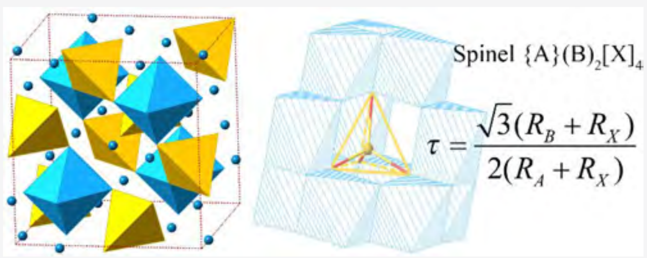

■ INTRODUCTION

The structural-descriptor-based approach has attracted much research attention in chemistry and materials science due to its potential applications in rapid estimation of phase stability and materials properties, with only a minimal calculation resource requirement compared to ab inito approaches.[1,2] Spinel-type compounds have aroused extensive research due to their prominent applications in electronics,[3] optics,[4,5] catalysis,[6,7] magnetism,[8,9] batteries,[10,11] and environmental protection.[12] With the general formula $\{A\}(B)_2[X]_4$, materials based on the spinel structure are able to accommodate a large variety of chemical elements, providing fascinating and diverse properties.[13−15] Therefore, developing the spinel-owned structural descriptor is urgent for materials design and discovery.[16]

The crystal structure of spinel belongs to space group $Fd\bar{3}m$.[17] It is known that the unit-cell has a constitution of 2 × 2 × 2 packed FCC (face centered cubic) cells, with anions X (O, S, Se) selected as the FCC lattice points. The {A} element occupies 1/8 of the tetrahedral (8 for 1 FCC cell) voids, while the (B) element occupies half of the octahedral (4 for 1 FCC cell) voids, as shown in Figure 1a. This structural description confirms the chemical formula of $\{A_{tet}\}$:(B_{oct}):[X] = 1:2:4, which is called normal spinel. In this work, only normal spinels are investigated, and other spinels, such as reverse and defected spinels, are beyond consideration. The site-occupancy preference is complex due to the composite influences of ionic radii, lattice energy, and ligand-field stabilization energies, etc. For example, in $\{Mg\}(Al)_2[O]_4$ it is the smaller Al^{3+} cation that occupies the larger octahedral site. Nevertheless, the spinel structure has diverse compositional candidates, including alkaline, alkaline earth, transition metal, rare earth, and chalcogen elements, which lead to large quantities of normal-spinel-type compounds. Bosi reports a strong correlation between the oxygen positional parameter (u) and the ionic potential (IP) by investigating the crystallographic data from

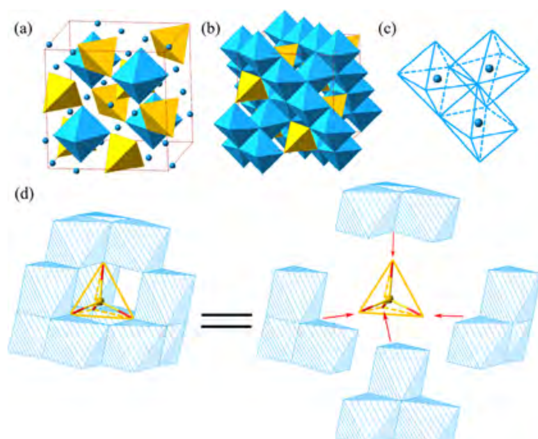

Figure 1. (a) Crystal structure of spinel. For clarity, the anions are hidden and only one-fourth of the octahedra are shown. (b) Connectivity between octahedra and tetrahedra. Since all the octahedra are shown, the triple octahedra units are noticeable. (c) Detailed illustration of the edge-sharing inside a triple octahedra unit. (d) Assembly of tetrahedron and triple octahedra units, showing the geometrical relationship between octahedron and tetrahedron.

Received: December 16, 2019
Revised: January 31, 2020
Published: February 13, 2020

Table 1. Tolerance Factor of AB_2X_4 Type Compounds[a]

ID Number	Formula	ICSD	τ
0812130	$\{Mg\}_1(Al)_2[O]_4$	167484	0.850
0812220	$\{Mg\}_1(Ti)_2[O]_4$	28324	0.910
0812230	$\{Mg\}_1(V)_2[O]_4$	56283	0.897
0812240	$\{Mg\}_1(Cr)_2[O]_4$	167459	0.886
0812390	$\{Mg\}_1(Y)_2[O]_4$	N.A.	1.013
0812450	$\{Mg\}_1(Rh)_2[O]_4$	109299	0.908
0814040	$\{Si\}_1(Be)_2[O]_4$	N.A.	0.966
0814120	$\{Si\}_1(Mg)_2[O]_4$	162406	1.109
0814200	$\{Si\}_1(Ca)_2[O]_4$	N.A.	1.257
0814260	$\{Si\}_1(Fe)_2[O]_4$	100552	1.051
0814280	$\{Si\}_1(Ni)_2[O]_4$	100544	1.093
0816030	$\{S\}_1(Li)_2[O]_4$	N.A.	1.236
0816190	$\{S\}_1(K)_2[O]_4$	N.A.	1.593
0820210	$\{Ca\}_1(Sc)_2[O]_4$	N.A.	0.811
0820710	$\{Ca\}_1(Lu)_2[O]_4$	N.A.	0.855
0823120	$\{V\}_1(Mg)_2[O]_4$	76980	0.988
0825130	$\{Mn\}_1(Al)_2[O]_4$	252228	0.813
0825220	$\{Mn\}_1(Ti)_2[O]_4$	22383	0.870
0825230	$\{Mn\}_1(V)_2[O]_4$	109148	0.858
0825240	$\{Mn\}_1(Cr)_2[O]_4$	167400	0.847
0825260	$\{Mn\}_1(Fe)_2[O]_4$	170910	0.819
0825450	$\{Mn\}_1(Rh)_2[O]_4$	109300	0.868
0825620	$\{Mn\}_1(Sm)_2[O]_4$	258904	0.993
0826130	$\{Fe\}_1(Al)_2[O]_4$	187920	0.825
0826230	$\{Fe\}_1(V)_2[O]_4$	109149	0.870
0826240	$\{Fe\}_1(Cr)_2[O]_4$	171121	0.860
0826260	$\{Fe\}_1(Fe)_2[O]_4$	162349	0.832
0826280	$\{Fe\}_1(Ni)_2[O]_4$	109150	0.836
0827130	$\{Co\}_1(Al)_2[O]_4$	290133	0.846
0827240	$\{Co\}_1(Cr)_2[O]_4$	61612	0.881
0827260	$\{Co\}_1(Fe)_2[O]_4$	198119	0.853
0827270	$\{Co\}_1(Co)_2[O]_4$	150805	0.851
0827450	$\{Co\}_1(Rh)_2[O]_4$	109301	0.904
0828130	$\{Ni\}_1(Al)_2[O]_4$	608815	0.859
0828240	$\{Ni\}_1(Cr)_2[O]_4$	28835	0.895
0828250	$\{Ni\}_1(Mn)_2[O]_4$	201398	0.879
0829130	$\{Cu\}_1(Al)_2[O]_4$	24491	0.850
0829250	$\{Cu\}_1(Mn)_2[O]_4$	174000	0.870
0830130	$\{Zn\}_1(Al)_2[O]_4$	163268	0.838
0830230	$\{Zn\}_1(V)_2[O]_4$	28963	0.884
0830240	$\{Zn\}_1(Cr)_2[O]_4$	167365	0.873
0830260	$\{Zn\}_1(Fe)_2[O]_4$	166205	0.844
0830310	$\{Zn\}_1(Ga)_2[O]_4$	187290	0.875
0830450	$\{Zn\}_1(Rh)_2[O]_4$	109298	0.894
0832260	$\{Ge\}_1(Fe)_2[O]_4$	93973	0.974
0832270	$\{Ge\}_1(Co)_2[O]_4$	21115	0.993
0832280	$\{Ge\}_1(Ni)_2[O]_4$	69508	1.013
0840120	$\{Zr\}_1(Mg)_2[O]_4$	N.A.	0.923
0842110	$\{Mo\}_1(Na)_2[O]_4$	44523	1.161
0842470	$\{Mo\}_1(Ag)_2[O]_4$	238013	1.224
0846300	$\{Pd\}_1(Zn)_2[O]_4$	30076	0.924
0848230	$\{Cd\}_1(V)_2[O]_4$	28961	0.810
0848240	$\{Cd\}_1(Cr)_2[O]_4$	197645	0.800
0848260	$\{Cd\}_1(Fe)_2[O]_4$	292074	0.774
0848260	$\{Cd\}_1(Fe)_2[O]_4$	619857	0.774
0848450	$\{Cd\}_1(Rh)_2[O]_4$	262941	0.820
0848490	$\{Cd\}_1(In)_2[O]_4$	4118	0.874
0874030	$\{W\}_1(Li)_2[O]_4$	N.A.	1.030
0874110	$\{W\}_1(Na)_2[O]_4$	2133	1.155
0912190	$\{Mg\}_1(K)_2[F]_4$	N.A.	1.239
1612210	$\{Mg\}_1(Sc)_2[S]_4$	37423	0.930
1612490	$\{Mg\}_1(In)_2[S]_4$	53096	0.950
1612700	$\{Mg\}_1(Yb)_2[S]_4$	37417	0.974
1612710	$\{Mg\}_1(Lu)_2[S]_4$	37420	0.972
1620570	$\{Ca\}_1(La)_2[S]_4$	N.A.	0.912
1620710	$\{Ca\}_1(Lu)_2[S]_4$	N.A.	0.857
1624310	$\{Cr\}_1(Ga)_2[S]_4$	626045	0.832
1625210	$\{Mn\}_1(Sc)_2[S]_4$	100832	0.896
1625240	$\{Mn\}_1(Cr)_2[S]_4$	164401	0.850
1625700	$\{Mn\}_1(Yb)_2[S]_4$	37418	0.939
1625710	$\{Mn\}_1(Lu)_2[S]_4$	37421	0.936
1626210	$\{Fe\}_1(Sc)_2[S]_4$	100527	0.907
1626240	$\{Fe\}_1(Cr)_2[S]_4$	291918	0.861
1626240	$\{Fe\}_1(Cr)_2[S]_4$	625932	0.861
1626260	$\{Fe\}_1(Fe)_2[S]_4$	194587	0.838
1626280	$\{Fe\}_1(Ni)_2[S]_4$	42590	0.841
1626450	$\{Fe\}_1(Rh)_2[S]_4$	174045	0.878
1626490	$\{Fe\}_1(In)_2[S]_4$	53488	0.926
1626700	$\{Fe\}_1(Yb)_2[S]_4$	37419	0.950
1626710	$\{Fe\}_1(Lu)_2[S]_4$	37422	0.948
1627240	$\{Co\}_1(Cr)_2[S]_4$	169878	0.879
1627270	$\{Co\}_1(Co)_2[S]_4$	24212	0.853
1627450	$\{Co\}_1(Rh)_2[S]_4$	174043	0.897
1628270	$\{Ni\}_1(Co)_2[S]_4$	24213	0.864
1628280	$\{Ni\}_1(Ni)_2[S]_4$	36271	0.870
1629220	$\{Cu\}_1(Ti)_2[S]_4$	44609	0.902
1629230	$\{Cu\}_1(V)_2[S]_4$	10035	0.891
1629240	$\{Cu\}_1(Cr)_2[S]_4$	196764	0.882
1629240	$\{Cu\}_1(Cr)_2[S]_4$	625758	0.882
1629270	$\{Cu\}_1(Co)_2[S]_4$	31107	0.857
1629450	$\{Cu\}_1(Rh)_2[S]_4$	291917	0.901
1629770	$\{Cu\}_1(Ir)_2[S]_4$	75531	0.906
1630130	$\{Zn\}_1(Al)_2[S]_4$	35380	0.843
1630240	$\{Zn\}_1(Cr)_2[S]_4$	166481	0.871
1630490	$\{Zn\}_1(In)_2[S]_4$	81811	0.938
1648130	$\{Cd\}_1(Al)_2[S]_4$	43025	0.784
1648210	$\{Cd\}_1(Sc)_2[S]_4$	94994	0.854
1648240	$\{Cd\}_1(Cr)_2[S]_4$	39415	0.811
1648490	$\{Cd\}_1(In)_2[S]_4$	108215	0.873
1648660	$\{Cd\}_1(Dy)_2[S]_4$	52798	0.910
1648670	$\{Cd\}_1(Ho)_2[S]_4$	246501	0.906
1648680	$\{Cd\}_1(Er)_2[S]_4$	100518	0.903
1648690	$\{Cd\}_1(Tm)_2[S]_4$	246502	0.899
1648700	$\{Cd\}_1(Yb)_2[S]_4$	246503	0.895
1648710	$\{Cd\}_1(Lu)_2[S]_4$	37410	0.893
1680240	$\{Hg\}_1(Cr)_2[S]_4$	53129	0.758
1680490	$\{Hg\}_1(In)_2[S]_4$	56081	0.816
1729550	$\{Cu\}_1(Cs)_2[Cl]_4$	N.A.	1.271
1730030	$\{Zn\}_1(Li)_2[Cl]_4$	202743	0.924
1730190	$\{Zn\}_1(K)_2[Cl]_4$	N.A.	1.149
3412390	$\{Mg\}_1(Y)_2[Se]_4$	76052	0.979
3412690	$\{Mg\}_1(Tm)_2[Se]_4$	76051	0.972
3412700	$\{Mg\}_1(Yb)_2[Se]_4$	76053	0.968
3412710	$\{Mg\}_1(Lu)_2[Se]_4$	44912	0.966
3425210	$\{Mn\}_1(Sc)_2[Se]_4$	74407	0.894
3425700	$\{Mn\}_1(Yb)_2[Se]_4$	76225	0.935
3429240	$\{Cu\}_1(Cr)_2[Se]_4$	43040	0.881
3429450	$\{Cu\}_1(Rh)_2[Se]_4$	41903	0.899
3430240	$\{Zn\}_1(Cr)_2[Se]_4$	150966	0.871
3430240	$\{Zn\}_1(Cr)_2[Se]_4$	626745	0.871
3448240	$\{Cd\}_1(Cr)_2[Se]_4$	241561	0.814
3448490	$\{Cd\}_1(In)_2[Se]_4$	52811	0.872

https://dx.doi.org/10.1021/acs.cgd.9b01673
Cryst. Growth Des. 2020, 20, 2014−2018

Table 1. continued

ID Number	Formula	ICSD	τ
3448660	$\{Cd\}_1(Dy)_2[Se]_4$	246499	0.908
3448670	$\{Cd\}_1(Ho)_2[Se]_4$	246500	0.904
3448690	$\{Cd\}_1(Tm)_2[Se]_4$	40582	0.898
3448700	$\{Cd\}_1(Yb)_2[Se]_4$	37408	0.894
3480240	$\{Hg\}_1(Cr)_2[Se]_4$	402408	0.763
3480240	$\{Hg\}_1(Cr)_2[Se]_4$	626175	0.763
5229240	$\{Cu\}_1(Cr)_2[Te]_4$	43041	0.880

[a]N.A. in the third column means no spinel phase is found in the ICSD database.

349 refined crystal structures.[18] Meanwhile, large values of u would lead to structural instability. However, this approach requires the knowledge of crystal structure. It still remains a great challenge to establish the relationship between chemical composition and the normal-spinel phase stability.

The tolerance factor is a useful tool to evaluate the phase stability of a certain crystal structure from initial chemical species. Usually, calculation of the tolerance factor only requires the empirical ionic radii of chemical components occupying different crystallographic sites in that structure. Goldschmidt established the tolerance factor for perovskite early in 1926,[19] and since then it has been continuously used as a guide in the discovery and research of perovskite compounds.[20] Similarly, the tolerance factor for garnets is set up as $\tau = \frac{3\sqrt{(R_B + R_D)^2 - \frac{4}{9}(R_A + R_D)^2}}{2(R_C + R_D)}$, where R_A, R_B, R_C, and R_D are ionic radii of chemical species occupying 24c, 16a, 24d, and 96h sites, respectively.[21] Kugimiya and Steinfink investigated the relationship between AB_2O_4 stoichiometries and their crystal structures.[22] They plotted diagrams relating the ratio of the radius of atom A/B to that of oxygen, as well as an artificial parameter derived from electronegativities. They also set up a tolerance factor based on the cubic cell geometry, i.e., the ratio $[110]/\sqrt{2}[100]$ but with no deep discussions.

Based on the consideration mentioned above, we put forward the tolerance factor for normal spinel in this work. On the assumption of hard-sphere packing of cations and anions, the geometrical relationships between octahedron and tetrahedron in the spinel structure are analyzed to express the tolerance factor using ionic radii of chemical species. Its validity is tested by taking more than 120 compounds with chemical formula AB_2X_4 into consideration. This structural descriptor could be combined with machine learning and high-throughput screening method to accelerate the discovery of novel spinel-type compounds.

■ METHODS

Connectivity between Octahedron and Tetrahedron in Spinel Structure. The traditional structural description of spinel in Figure 1a clearly demonstrates the quantitative relationship between octahedron and tetrahedron. On the other hand, when the spinel structure is examined for connectivity with all the octahedra shown in Figure 1b, the existence of a triple octahedra unit is readily recognizable. It is formed by three octahedra sharing two edges with each other, as shown in Figure 1c. As a result, there exists a common vertex shared by all the constituting octahedra. From the assembly scheme in Figure 1d, it is clearly seen that one tetrahedron is confined in a cage formed by edge-sharing triple octahedra units with their common vertexes as the linking points. This viewpoint provides a more straightforward way to present the geometrical relationship between octahedron and tetrahedron in the spinel structure.

Setting Up Tolerance Factor by Ionic Radii. Investigation of Figure 1d reveals a quantitative geometrical relationship; i.e., the height of tetrahedron enclosed is equal to the distance between two parallel triangular planes of octahedron. Meanwhile, on the assumption of hard-sphere packing, the quantities mentioned above can be expressed with the help of ionic radii. After simple solid geometrical calculations, the octahedral interplanar distance can be expressed as $L' = 2\sqrt{(R_B + R_X)^2 - \left(\frac{\sqrt{3}}{3}L\right)^2}$, where $L = \sqrt{2}(R_B + R_X)$ is the edge length of the ocatahedron. Similarly, the height H of tetrahedron with edge length L'' is $H = \sqrt{\frac{2}{3}}L''$, where $L'' = \sqrt{\frac{8}{3}}(R_A + R_X)$. Finally, the ratio between L' and H is selected to represent the tolerance factor τ, which is

$$\tau = \frac{L'}{H} = \frac{2\sqrt{(R_B + R_X)^2 - \frac{2}{3}(R_B + R_X)^2}}{\sqrt{\frac{2}{3}} \times \sqrt{\frac{8}{3}}(R_A + R_X)} = \frac{\sqrt{3}(R_B + R_X)}{2(R_A + R_X)}$$

Therefore, the ionic radii of all the constituent chemical elements are included in the expression of τ, and the numerical values of real spinel-type compounds are expected to fluctuate around 1.

■ RESULTS AND DISCUSSION

Tolerance Factor Survey of Spinel Structures with Different Chemical Species. To test the validity of tolerance factor in characterizing the phase stability of normal spinel, more than 120 compounds with chemical formula AB_2X_4 are examined. The phase identification is checked from ICSD (Inorganic Crystal Structure Database),[23] and only those present at ambient pressure and room temperature are considered. For the calculation of τ, the Shannon ionic radii[24,25] of the constituting chemical species are selected in accordance with the coordination number (CN), i.e., CN = 4 for $\{A_{tet}\}$, CN = 6 for (B_{oct}), and CN = 4 for [X]. In several cases, the ionic radii data for CN = 4 is unavailable (Ca^{2+}, Pd^{4+}, Cl^-, S^{2-}, etc.), and the values are obtained from ionic radii of CN = 6 multiplied by a coefficient. For cations, the coefficient is $\frac{0.88}{0.96} = 0.916$, which equals the statistical ratio between the relative atomic radii of metals with CN = 4 and CN = 6, whereas for anions, the atomic radii changes less sensitively with regard to coordination number, and the coefficient is selected as 0.985, which is the ratio belonging to O and F.[24] At the same time, we ascribe every compound with an identification number according to the chemical formula. The atomic number of element at [X] occupies the first two digits, i.e., 08 for O, 16 for S, and 34 for Se. The next two digits belong to the chemical element at {A} and the following two for (B). The last digit is reserved to distinguish the normal and reverse spinels in the future. For now, it is set as zero for normal spinels. The identification number, chemical formula, ICSD code, and τ values are compiled in Table 1. The scatter plot of τ is shown in Figure 2, where nonspinel phases are denoted by crossed purple circles, and exceptions by black pentagrams. They will be discussed in detail later.

Crystal Chemistry of Spinel Compounds in View of Tolerance Factor. A broad view of Figure 2 confirms the validity of spinel-owned tolerance factor in evaluating the

https://dx.doi.org/10.1021/acs.cgd.9b01673
Cryst. Growth Des. 2020, 20, 2014−2018

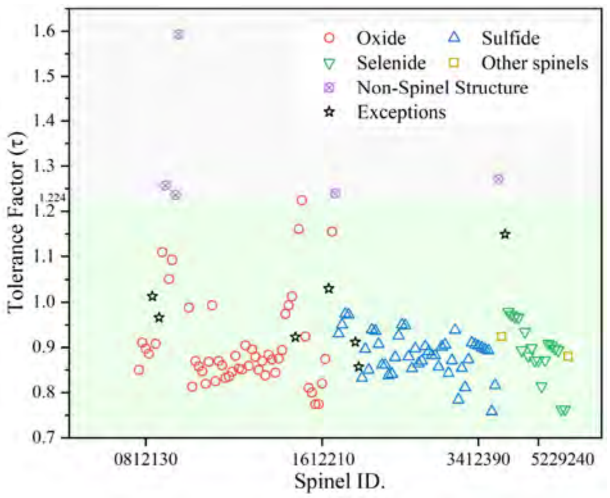

Figure 2. Survey of the tolerance factor τ for normal spinel structures.

phase stability from given chemical species. The τ values are scattered around 1 as expected, while the major part is located in the neighborhood of 0.85. This discrepancy reflects internal stress exerted on (B_{oct}) sites, since it is the octahedral framework that supports the spinel structure. As a result, the smaller nominator leads to tolerance factor less than 1. A large τ value makes the spinel phase unstable, as indicated by the crossed purple circles in Figure 2. Although those compounds share the chemical formula of AB_2X_4, the polyhedral connectivity differs from the typical $MgAl_2O_4$ structure (Figure 3a−d). Even for K_2MgF_4 and Li_2SO_4, the CN increases from 4

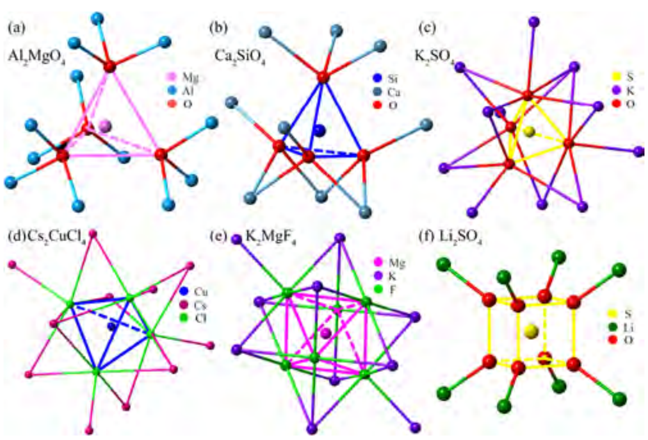

Figure 3. Crystal structure comparison between typical spinel $MgAl_2O_4$ (a) and those nonspinel AB_2X_4 compounds Ca_2SiO_4 (b), K_2SO_4 (c), Cs_2CuCl_4 (d), K_2MgF_4 (e), and Li_2SO_4 (e).

to 6 and 8, respectively, in Figure 3e,f. Therefore, it is expected that the AB_2X_4 type compounds have more chance to crystallize in the spinel phase with a τ value close to 1. However, there are shortcomings for this tolerance factor to deal with exceptions. Several AB_2X_4 stoichiometry compounds with appropriate numerical values have nonspinel structures, such as ZnK_2Cl_4 (1730190, τ = 1.149), WLi_2O_4 (0874030, τ = 1.030), and $SiBe_2O_4$ (0814040, τ = 0.966). Meanwhile, in ternary Mg−Y−O, Mg−Zr−O, and Zr−In−O systems, up to now no compounds have been reported to crystallize in spinel structures, or even with AB_2X_4 stoichiometries such as MgY_2O_4 and $ZrMg_2O_4$. It also fails in predicting the spinel-phase stability for oxide or sulfide containing calcium and lanthanides. $CaSc_2O_4$ (0820210, τ = 0.811), $CaLu_2O_4$ (0820710, τ = 0.855), and $CaLu_2S_4$ (1620710, τ = 0.857) have orthorhombic space group *Pnam*, while $CaLa_2S_4$ (1620570, τ = 0.912) has space group $I\bar{4}3d$. Those compounds all have appropriate values of tolerance factor, but crystallized in structures deviated from spinel. The reason lies in that the 4-coordinated environment in the spinel structure is too small for Ca to occupy, and in $CaLn_2X_4$ compounds the coordination number is 7 or 8. As mentioned above, the Shannon radii for Ca with CN = 4 is unavailable, and the value is set at about 0.9 of that with CN = 6 for tolerance factor calculation. Therefore, this method may be improved by adopting a smaller coefficient, which can increase the tolerance factor values to the exclusion region.

■ CONCLUSIONS

In this work, the tolerance factor of the normal spinel structure is established on the basis of polyhedral geometry. A survey of more than 120 compounds with chemical formula AB_2X_4 supports the validity of the tolerance factor on predicting the phase stability of normal spinel structure. The data is scattered around 0.85, because the octahedra are compressed to constitute the main framework of spinel structure. It is expected to serve as a useful structural descriptor in machine learning and high-throughput screening applications for material property evaluation and novel spinel-type compound discovery.

■ AUTHOR INFORMATION

Corresponding Author

Quanlin Liu − *Beijing Key Laboratory for New Energy Materials and Technologies, School of Materials Science and Engineering, University of Science and Technology Beijing, Beijing 100083, China;* orcid.org/0000-0003-3533-7140; Email: qlliu@ustb.edu.cn

Author

Zhen Song − *Beijing Key Laboratory for New Energy Materials and Technologies, School of Materials Science and Engineering, University of Science and Technology Beijing, Beijing 100083, China;* orcid.org/0000-0002-7251-5703

Complete contact information is available at:
https://pubs.acs.org/10.1021/acs.cgd.9b01673

Notes

The authors declare no competing financial interest.

■ ACKNOWLEDGMENTS

This work is supported by the National Natural Science Foundation of China (No. 51832005 and 51602019).

■ REFERENCES

(1) Jain, A.; Voznyy, O.; Sargent, E. H. High-Throughput Screening of Lead-Free Perovskite-like Materials for Optoelectronic Applications. *J. Phys. Chem. C* **2017**, *121*, 7183−7187.

(2) Zhao, X.-G.; Yang, J.-H.; Fu, Y.; Yang, D.; Xu, Q.; Yu, L.; Wei, S.-H.; Zhang, L. Design of Lead-Free Inorganic Halide Perovskites for Solar Cells via Cation-Transmutation. *J. Am. Chem. Soc.* **2017**, *139*, 2630−2638.

(3) Wei, T.-Y.; Chen, C.-H.; Chien, H.-C.; Lu, S.-Y.; Hu, C.-C. A Cost-Effective Supercapacitor Material of Ultrahigh Specific Capaci-

tances: Spinel Nickel Cobaltite Aerogels from an Epoxide-Driven Sol-Gel Process. *Adv. Mater.* **2010**, *22*, 347−351.

(4) Abraham, A. G.; Manikandan, A.; Manikandan, E.; Vadivel, S.; Jaganathan, S. K.; Baykal, A.; Renganathan, P. S. Enhanced Magneto-Optical and Photo-Catalytic Properties of Transition Metal Cobalt (Co^{2+} Ions) Doped Spinel $MgFe_2O_4$ Ferrite Nanocomposites. *J. Magn. Magn. Mater.* **2018**, *452*, 380−388.

(5) Horng, R.-H.; Huang, C.-Y.; Ou, S.-L.; Juang, T.-K.; Liu, P.-L. Epitaxial Growth of $ZnGa_2O_4$: A New, Deep Ultraviolet Semiconductor Candidate. *Cryst. Growth Des.* **2017**, *17*, 6071−6078.

(6) Cheng, F.; Shen, J.; Peng, B.; Pan, Y.; Tao, Z.; Chen, J. Rapid Room-Temperature Synthesis of Nanocrystalline Spinels as Oxygen Reduction and Evolution Electrocatalysts. *Nat. Chem.* **2011**, *3*, 79−84.

(7) Liang, Y.; Wang, H.; Zhou, J.; Li, Y.; Wang, J.; Regier, T.; Dai, H. Covalent Hybrid of Spinel Manganese-Cobalt Oxide and Graphene as Advanced Oxygen Reduction Electrocatalysts. *J. Am. Chem. Soc.* **2012**, *134*, 3517−3523.

(8) Sonia, M. M. L.; Anand, S.; Vinosel, V. M.; Janifer, M. A.; Pauline, S.; Manikandan, A. Effect of Lattice Strain on Structure, Morphology and Magneto-Dielectric Properties of Spinel $NiGd_xFe_{2-x}O_4$ Ferrite Nano-Crystallites Synthesized by Sol-Gel Route. *J. Magn. Magn. Mater.* **2018**, *466*, 238−251.

(9) Katayama, T.; Kurauchi, Y.; Mo, S.; Gu, K.; Chikamatsu, A.; Galiullina, L.; Hasegawa, T. P-Type Conductivity and Room-Temperature Ferrimagnetism in Spinel $MoFe_2O_4$ Epitaxial Thin Film. *Cryst. Growth Des.* **2019**, *19*, 902−906.

(10) Gu, M.; Belharouak, I.; Zheng, J.; Wu, H.; Xiao, J.; Genc, A.; Amine, K.; Thevuthasan, S.; Baer, D. R.; Zhang, J.-G.; Browning, N. D.; Liu, J.; Wang, C. Formation of the Spinel Phase in the Layered Composite Cathode Used in Li-Ion Batteries. *ACS Nano* **2013**, *7*, 760−767.

(11) Zhao, D.; Dai, M.; Liu, H.; Xiao, L.; Wu, X.; Xia, H. Constructing High Performance Hybrid Battery and Electrocatalyst by Heterostructured $NiCo_2O_4$@NiWS Nanosheets. *Cryst. Growth Des.* **2019**, *19*, 1921−1929.

(12) Yang, Y.; Liu, J.; Zhang, B.; Liu, F. Mechanistic Studies of Mercury Adsorption and Oxidation by Oxygen over Spinel-Type $MnFe_2O_4$. *J. Hazard. Mater.* **2017**, *321*, 154−161.

(13) Li, C.; Han, X.; Cheng, F.; Hu, Y.; Chen, C.; Chen, J. Phase and Composition Controllable Synthesis of Cobalt Manganese Spinel Nanoparticles towards Efficient Oxygen Electrocatalysis. *Nat. Commun.* **2015**, *6*, 7345.

(14) Wang, H.-Y.; Hung, S.-F.; Chen, H.-Y.; Chan, T.-S.; Chen, H. M.; Liu, B. In Operando Identification of Geometrical-Site-Dependent Water Oxidation Activity of Spinel Co_3O_4. *J. Am. Chem. Soc.* **2016**, *138*, 36−39.

(15) Talanov, M. V. Two Different Mechanisms of Metal Cluster Formation in the Rhombohedral Spinel Structures: AlV_2O_4 and $CuZr_{1.86(1)}S_4$. *Cryst. Growth Des.* **2018**, *18*, 3433−3440.

(16) Wei, C.; Feng, Z.; Scherer, G. G.; Barber, J.; Shao-Horn, Y.; Xu, Z. J. Cations in Octahedral Sites: A Descriptor for Oxygen Electrocatalysis on Transition-Metal Spinels. *Adv. Mater.* **2017**, *29*, 1606800.

(17) Zhao, Q.; Yan, Z.; Chen, C.; Chen, J. Spinels: Controlled Preparation, Oxygen Reduction/Evolution Reaction Application, and Beyond. *Chem. Rev.* **2017**, *117*, 10121−10211.

(18) Bosi, F. Chemical and Structural Variability in Cubic Spinel Oxides. *Acta Crystallogr., Sect. B: Struct. Sci., Cryst. Eng. Mater.* **2019**, *75*, 279−285.

(19) Goldschmidt, V. M. Die Gesetze Der Krystallochemie. *Naturwissenschaften* **1926**, *14*, 477−485.

(20) Song, Z.; Zhao, J.; Liu, Q. L. Luminescent Perovskites: Recent Advances in Theory and Experiments. *Inorg. Chem. Front.* **2019**, *6*, 2969−3011.

(21) Song, Z.; Zhou, D. D.; Liu, Q. L. Tolerance Factor and Phase Stability of the Garnet Structure. *Acta Crystallogr., Sect. C: Struct. Chem.* **2019**, *75*, 1353−1358.

(22) Kugimiya, K.; Steinfink, H. Influence of Crystal Radii and Electronegativities on the Crystallization of AB_2X_4 Stoichiometries. *Inorg. Chem.* **1968**, *7*, 1762−1770.

(23) Bergerhoff, G.; Brown, I. D. In *Crystallographic Databases*, Allen, F. H.; Bergerhoff, G.; Sievers, R., Eds.; International Union of Crystallography: Chester, 1987.

(24) Shannon, R. D.; Prewitt, C. T. Effective Ionic Radii in Oxides and Fluorides. *Acta Crystallogr., Sect. B: Struct. Crystallogr. Cryst. Chem.* **1969**, *25*, 925−946.

(25) Shannon, R. D. Revised Effective Ionic Radii and Systematic Studies of Interatomic Distances in Halides and Chalcogenides. *Acta Crystallogr., Sect. A: Cryst. Phys., Diffr., Theor. Gen. Crystallogr.* **1976**, *32*, 751−767.